

AB598, a Therapeutic Anti-Human CD39 Antibody, Binds and Inhibits CD39 Enzymatic Activity *In Vivo* to Promote Anti-Tumor Immunity



Kaustubh Parashar, Julie Clor, Amy E. Anderson, Urvi Vani, Jaskirat Singh, Enzo Stagnaro, Ferdie Soriano, Angelo Kaplan, Janine Kline, Lisa Seitz, Stephen W. Young, Nigel P. Walker, Matthew J. Walters, Ester Fernandez-Salas, Christine E. Bowman

Arcus Biosciences, Inc.; 3928 Point Eden Way, Hayward, CA 94545 (USA)

SITC Annual Meeting
Nov. 8-12, 2022
Abstract 991

INTRODUCTION

- AB598, which potently binds and inhibits CD39 enzymatic activity, is being developed as a cancer immunotherapy. CD39 catalyzes the conversion of extracellular adenosine triphosphate (ATP) into adenosine monophosphate (AMP), resulting in decreased amounts of immunostimulatory ATP and increased levels of immunosuppressive adenosine in the tumor microenvironment (TME). By blocking CD39 in the TME, local levels of ATP increase, leading to myeloid cell activation and improved tumor control.
- AB598 is highly potent and specific, binding and inhibiting human CD39 with sub-nanomolar potency. AB598 does not bind or inhibit murine CD39, presenting a challenge for studying CD39 inhibition in an immunocompetent syngeneic tumor model. Human CD39 knock-in (hCD39KI) mice were employed to examine the preclinical anti-tumor efficacy of AB598 in animals with a fully competent immune system. The use of a murine model with natural expression and distribution of human CD39, targetable by AB598, allowed for a more physiological assessment of CD39 inhibition in solid tumors compared to the alternative use of human cancer cells growing in immunodeficient mice.

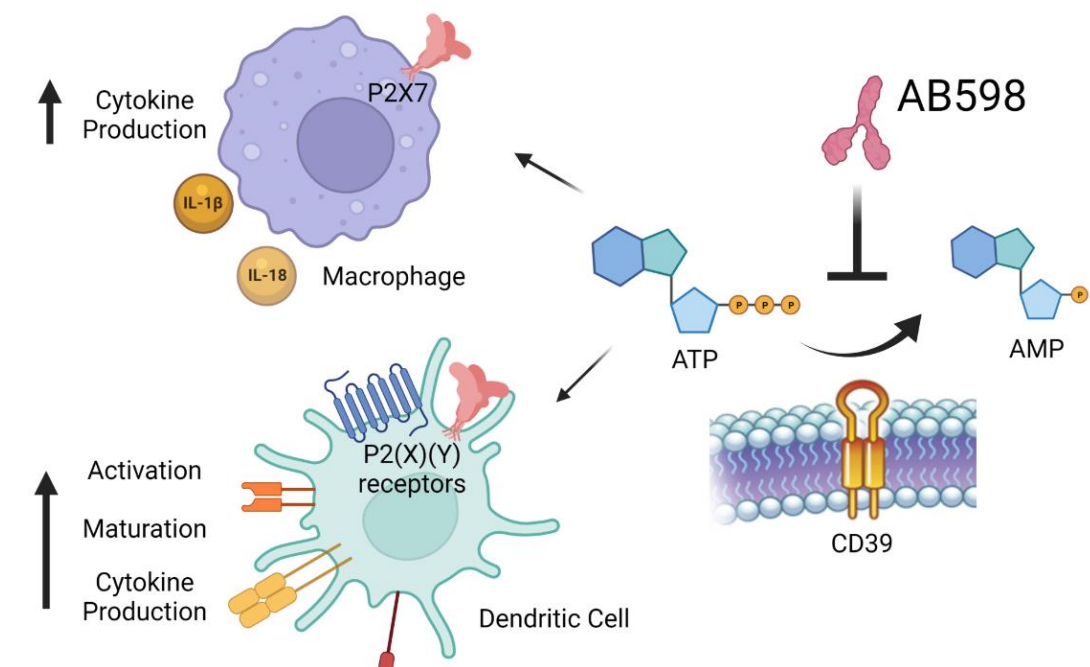


Figure 1. CD39 inhibition promotes anti-tumor immunity by promoting myeloid cell activation. Schematic created with BioRender.com.

RESULTS

AB598 Bolsters Extracellular ATP in Combination With Oxaliplatin

Oxaliplatin Induces the Hallmarks of ICD

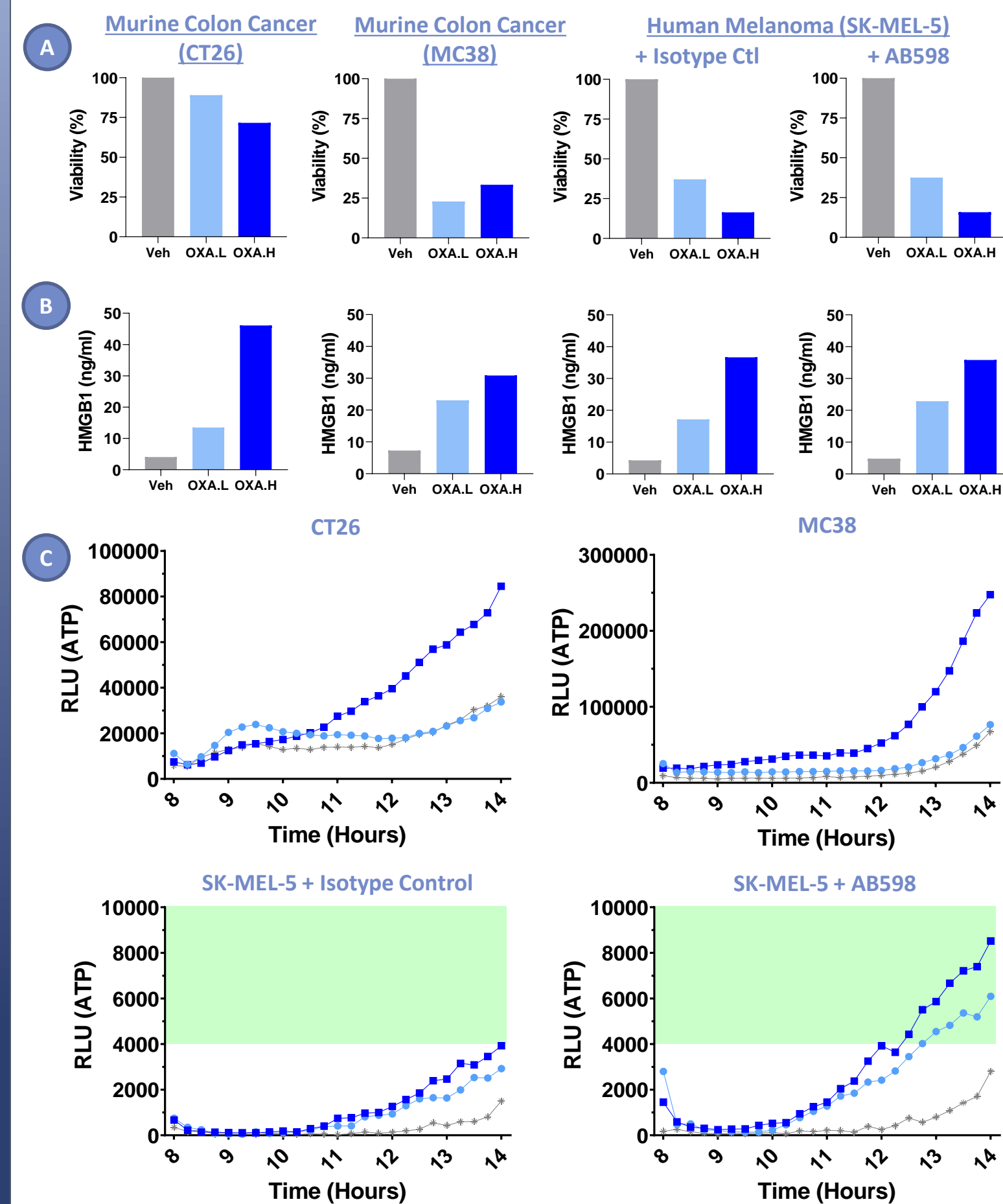


Figure 2. Oxaliplatin (OXA) induces ICD and ATP release in cancer cell lines used for *in vivo* tumor models. CT26, MC38, and SK-MEL-5 cell lines were treated with OXA at two concentrations, 100 μM (OXA.L) or 250 μM (OXA.H). (A) After 24 hours, cellular viability was measured using the Promega Cell Titer Glo assay. (B) After 24 hours, HMGB1 levels in the culture supernatant were measured using the Promega Lumit HMGB1 assay. (C) To measure extracellular ATP, cells were treated with the indicated amount of OXA and in the case of SK-MEL-5, 100 nM AB598 or a matched Fc-silent IgG1 isotype control for 8 hours. Extracellular ATP levels were measured over the following 6 hours using Promega RealTime Glo Extracellular ATP assay. OXA, an ICD-inducer, causes cell death, HMGB1 release, and extracellular ATP release in all three cell lines tested. Treatment of SK-MEL-5 cells with AB598 increased the amount of extracellular ATP in the cell culture supernatant as compared to the isotype control treated cells. AB598 treatment did not affect SK-MEL-5 cell viability or HMGB1 release (data not shown).

Human CD39 Knock-In Mice are an Immunocompetent Model Amenable to CD39 Inhibition

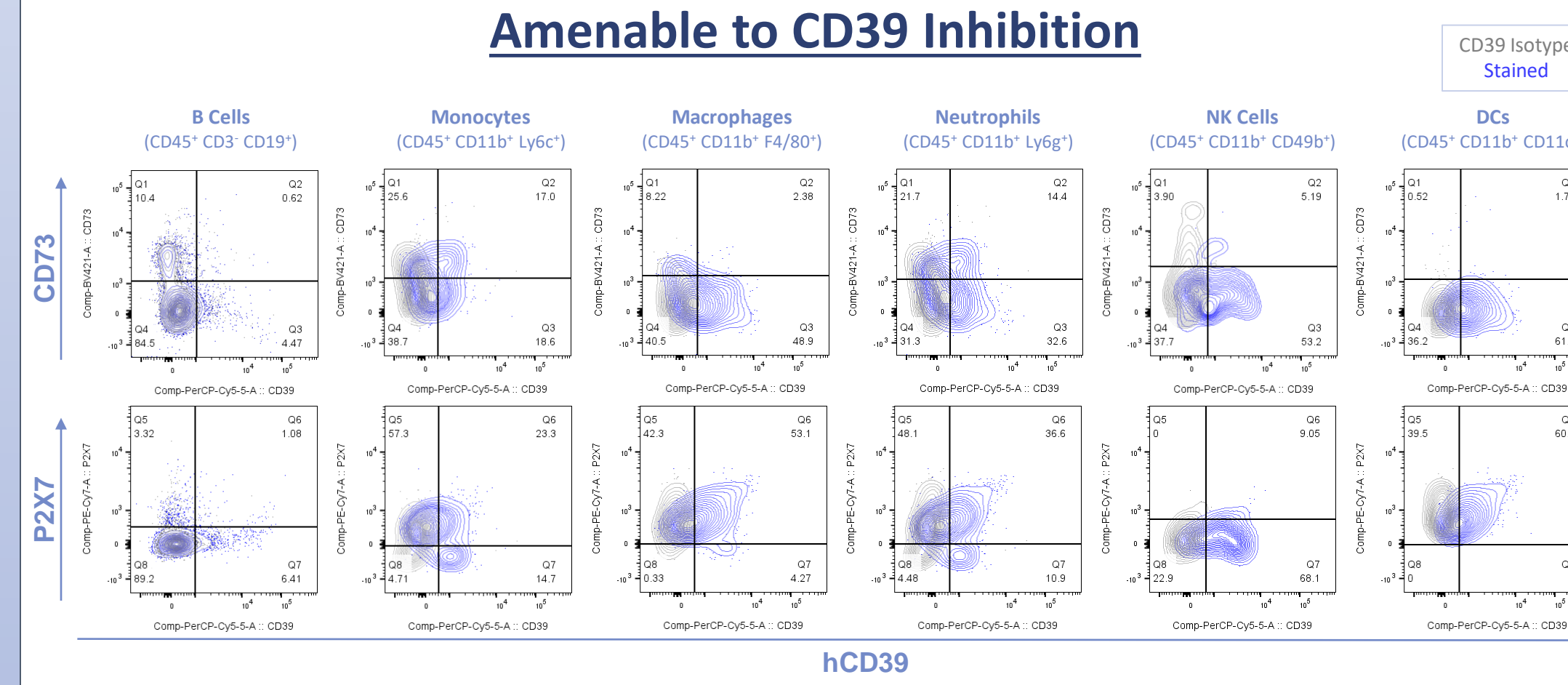


Figure 3. Expression of CD39, CD73, and P2X7 on immune cells from hCD39KI mice. Flow plots showing the distribution of human CD39, mouse CD73, and mouse P2X7 on immune cells from the lymph nodes of isotype control treated mice collected at the end of the study shown in Figure 4. The tumor draining lymph nodes were removed, dissociated and analyzed by flow cytometry for expression of cell surface CD39, CD73, and P2X7. Gates were set on isotype controls (hCD39 isotype control in grey) and applied to each group (blue). A natural distribution of immune cell populations and CD39, CD73, and P2X7 expression was observed in the hCD39KI model.

AB598.mlgG2a + OXA Combination Shows Efficacy Compared to Single Agents in a C57BL/6 hCD39KI MC38 Model

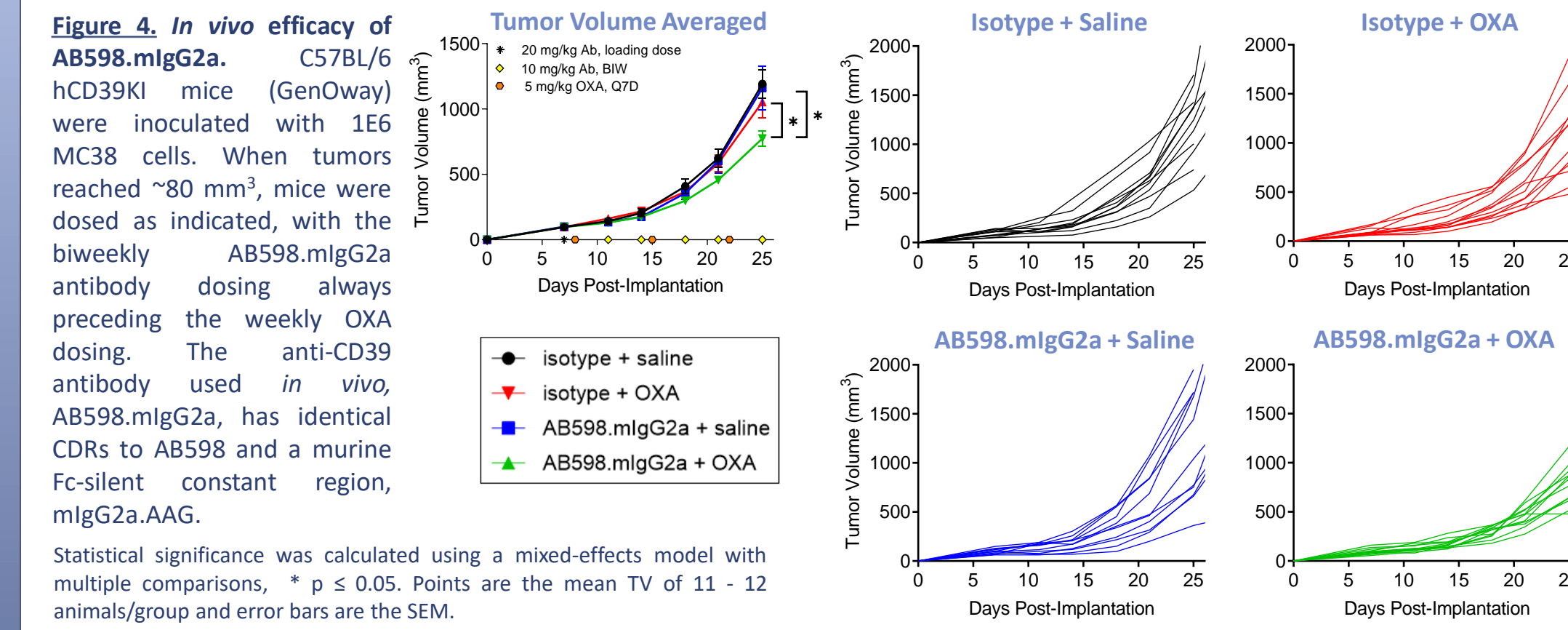


Figure 4. *In vivo* efficacy of AB598.mlgG2a. C57BL/6 hCD39KI mice (GenOway) were inoculated with 1E6 MC38 cells. When tumors reached ~80 mm³, mice were dosed as indicated, with the biweekly AB598.mlgG2a antibody dosing always preceding the weekly OXA dosing. The anti-CD39 antibody used *in vivo*, AB598.mlgG2a, has identical CDRs to AB598 and a murine Fc-silent constant region, mlgG2a.AAG. Statistical significance was calculated using a mixed-effects model with multiple comparisons, * p ≤ 0.05. Points are the mean TV of 11 - 12 animals/group and error bars are the SEM.

Peripheral Blood from hCD39KI Mice Treated with AB598.mlgG2a Shows Full Receptor Occupancy

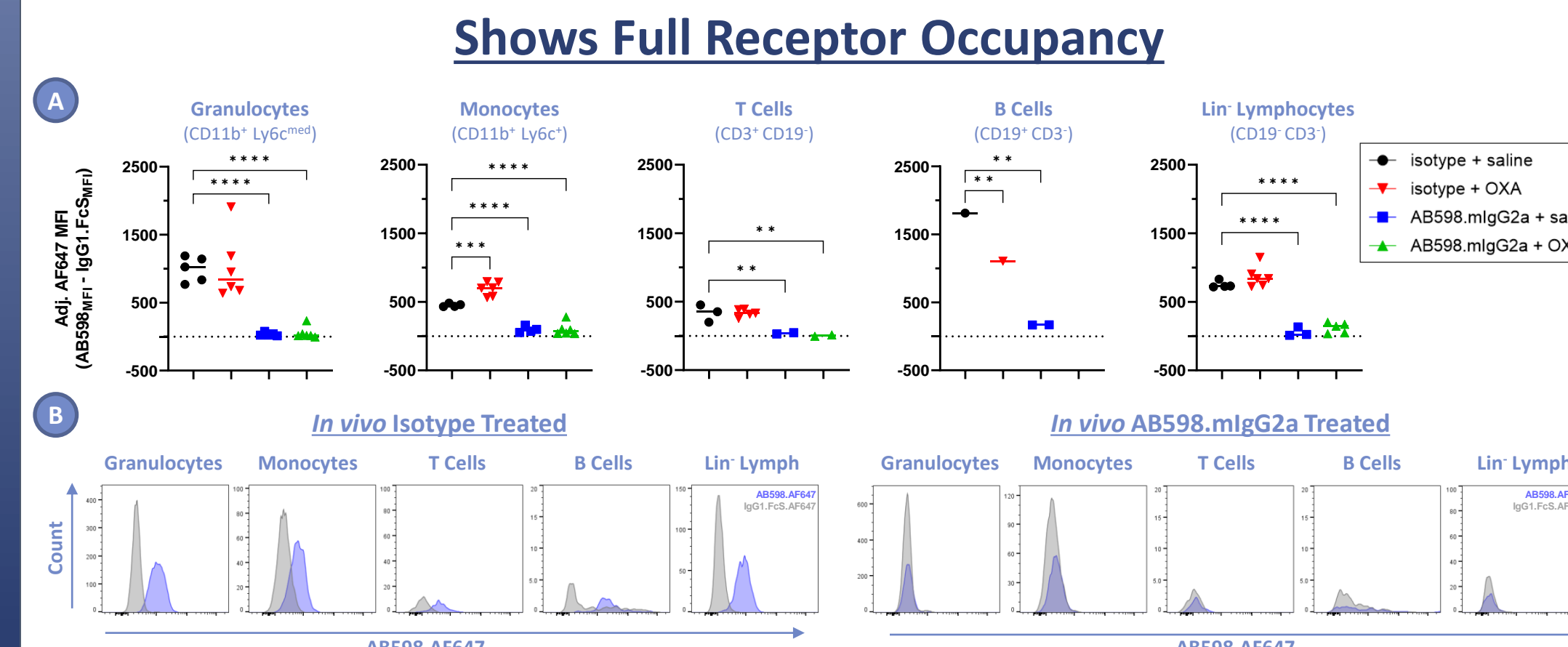


Figure 5. Complete target coverage observed with AB598.mlgG2a treatment in peripheral immune populations. Whole blood from terminal bleeds from the study shown in Figure 4 was assessed by flow cytometry for receptor occupancy. (A) Binding of a competitive antibody, AB598.AF647, was observed on all CD39(A1)-expressing cells in the *in vivo* isotype control treated mice, but not on the CD39(A1)-expressing cells in the *in vivo* AB598.mlgG2a treated mice, indicating complete or near-complete target coverage. Data are shown for populations where >100 CD39(A1)⁺ events were collected. (B) Representative histograms from mice treated *in vivo* with either isotype or AB598.mlgG2a. Statistical analysis was performed with One-way ANOVA (Dunnett's multiple comparison test, with a single pooled variance), * p ≤ 0.05, ** p ≤ 0.01, *** p ≤ 0.001, **** p ≤ 0.0001.

AB598.mlgG2a Inhibits Intratumoral and Peripheral CD39 Enzymatic Activity *In Vivo*

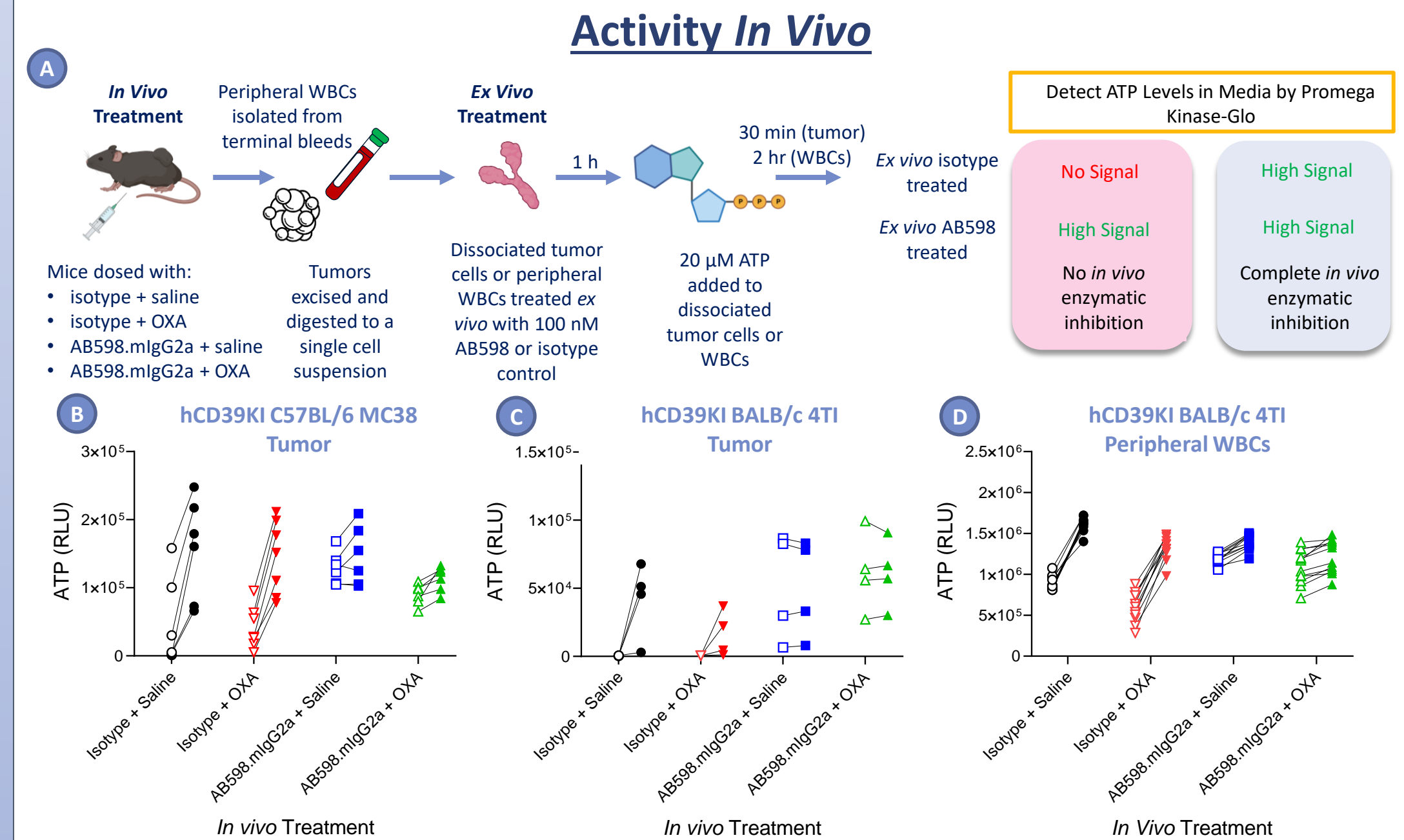


Figure 6. AB598 inhibits intratumoral and peripheral CD39 *in vivo*. Mice bearing MC38 (B) or 4T1 (C,D) tumors were treated *in vivo* as described in Figure 4. At the end of the study, tumors were collected and assayed for CD39 enzymatic activity. The difference between *ex vivo* 100 nM isotype (open shapes) and 100 nM AB598 (filled shapes) is evidence of residual enzymatic activity that was not inhibited by *in vivo* treatment. Complete or near complete enzymatic inhibition was achieved in all tumors where mice were treated with AB598.mlgG2a.

CD39 Is Inhibited in Tumors and Spleens of hCD39KI Mice

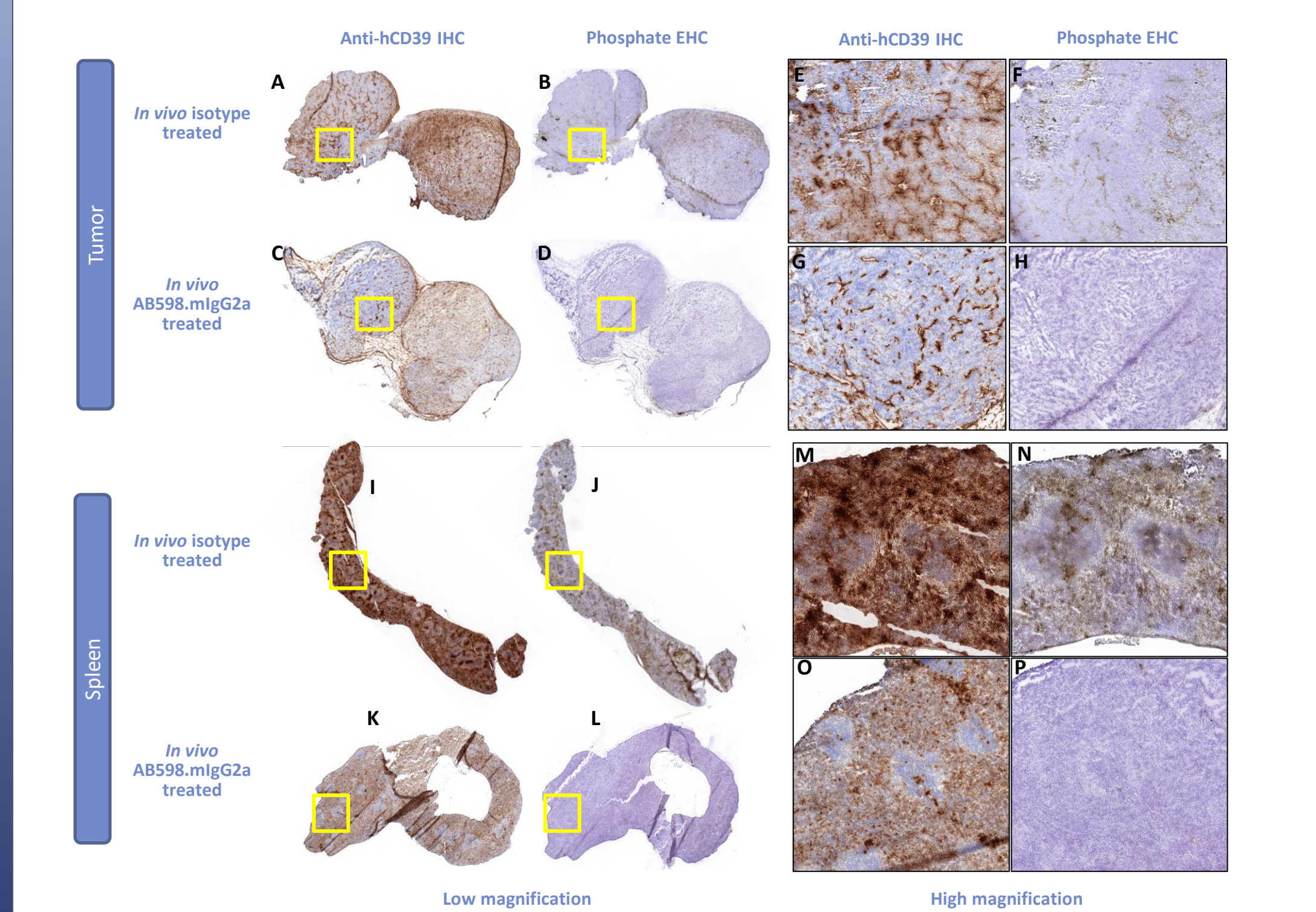


Figure 7. Tumors and spleens from hCD39KI mice show human CD39 expression and activity that is inhibited with AB598.mlgG2a treatment. Tumors and spleens from mice at the end of the study shown in Figure 4 were analyzed for hCD39 expression by immunohistochemistry (IHC) and evidence of AB598.mlgG2a blocking enzymatic activity by enzyme histochemistry (EHC). The EHC assay was conducted in the presence of 1 mM ATP substrate and 2.5 mM levamisole (to block non-specific phosphatase activity). Human CD39 expression was detected in both isotype treated (A and E) and AB598.mlgG2a treated tumors (C and G), localized to vascular endothelia, infiltrating immune cells, and stromal components of the TME. Human CD39 expression was observed in both isotype treated (I and M) and AB598.mlgG2a treated spleens (K and O), localized to the red pulp and to a lesser degree in the white pulp. In tumors and spleens treated *in vivo* with isotype control antibody, lead-phosphate deposition is observed by EHC (B and F tumor, J and N spleen). In tumors and spleens treated *in vivo* with AB598.mlgG2a, lead-phosphate deposition is not observed by EHC, indicating that enzymatic activity has been blocked (D and H tumor, L and P spleen).

Peripheral Blood from hCD39KI Mice Treated with AB598.mlgG2a Shows a Decrease in Cell Surface CD39

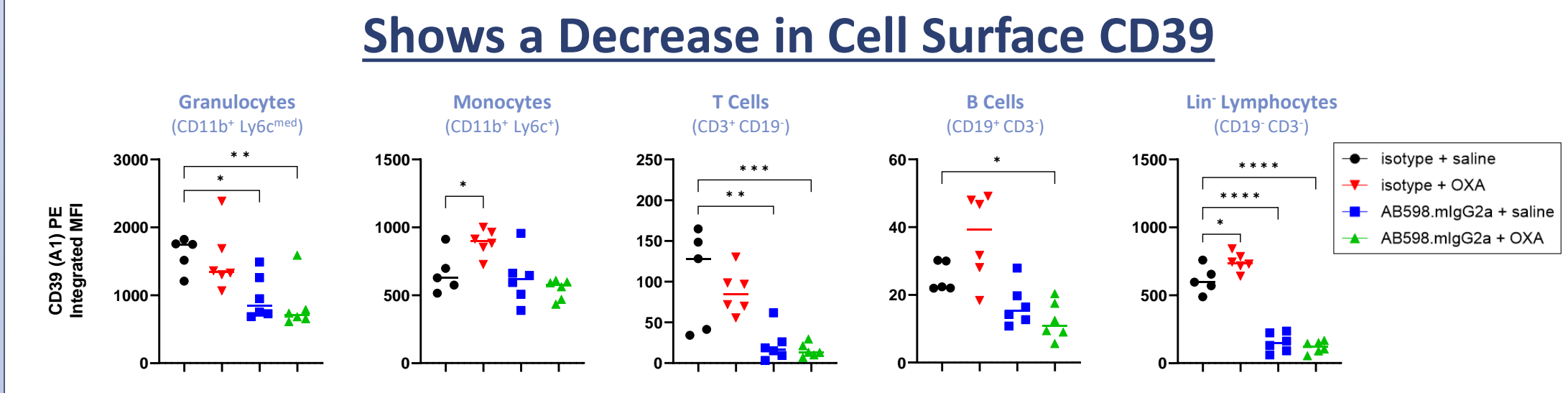


Figure 8. Decrease in cell surface CD39 observed with *in vivo* AB598.mlgG2a treatment in peripheral immune populations. Whole blood from terminal bleeds from the study shown in Figure 4 was assessed by flow cytometry for total CD39 surface expression. A decrease in cell surface CD39 expression, determined by binding of the non-competitive anti-CD39 clone A1-PE, was observed in multiple cell types after *in vivo* AB598.mlgG2a treatment. Statistical analysis was performed with One-way ANOVA (Dunnett's multiple comparison test, with a single pooled variance), * p ≤ 0.05, ** p ≤ 0.01, *** p ≤ 0.001, **** p ≤ 0.0001.

Surface Expression of CD39 Decreases with AB598.mlgG2a Treatment in Tumor Draining Lymph Nodes

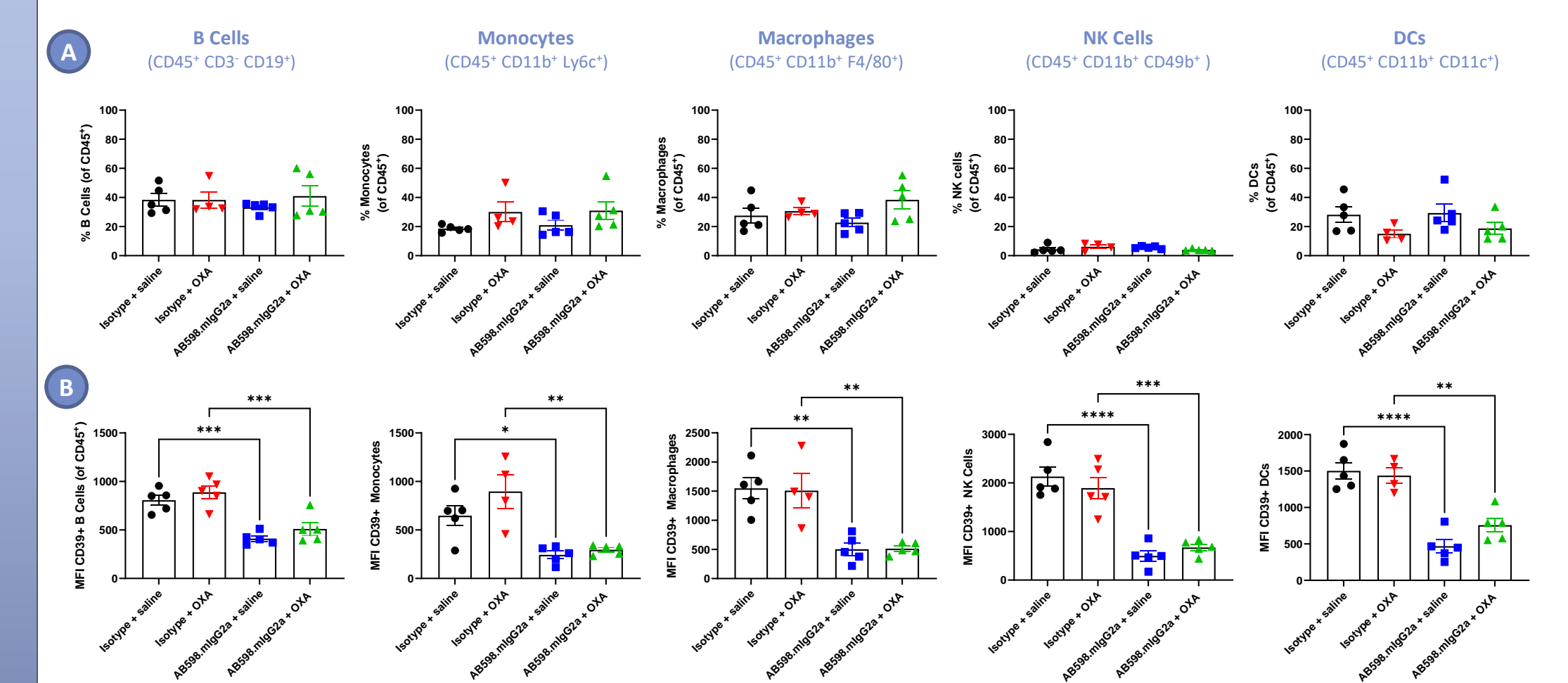


Figure 9. Cell surface CD39 decreases with AB598.mlgG2a treatment in tumor draining lymph nodes of hCD39KI mouse model. The tumor draining lymph nodes (inguinal lymph nodes on tumor-bearing side) from mice inoculated with MC38 tumors were removed, dissociated and analyzed by flow cytometry for expression of cell surface CD39 at the conclusion of the experiment shown in Figure 4. Statistical analysis was performed with a One-way ANOVA (Dunnett's multiple comparison test, with a single pooled variance), * p ≤ 0.05, ** p ≤ 0.01, *** p ≤ 0.001, **** p ≤ 0.0001, bar height is the mean and error bars are +/- SEM. There was no significant change in immune subpopulation percentages observed with AB598.mlgG2a treatment (A), but a significant decrease in CD39 cell surface expression was observed with AB598.mlgG2a treatment in almost all immune sub-populations (B).

Peripheral Cytokines Are Unaffected by AB598.mlgG2a Treatment in a C57BL/6 hCD39KI MC38 Tumor Model

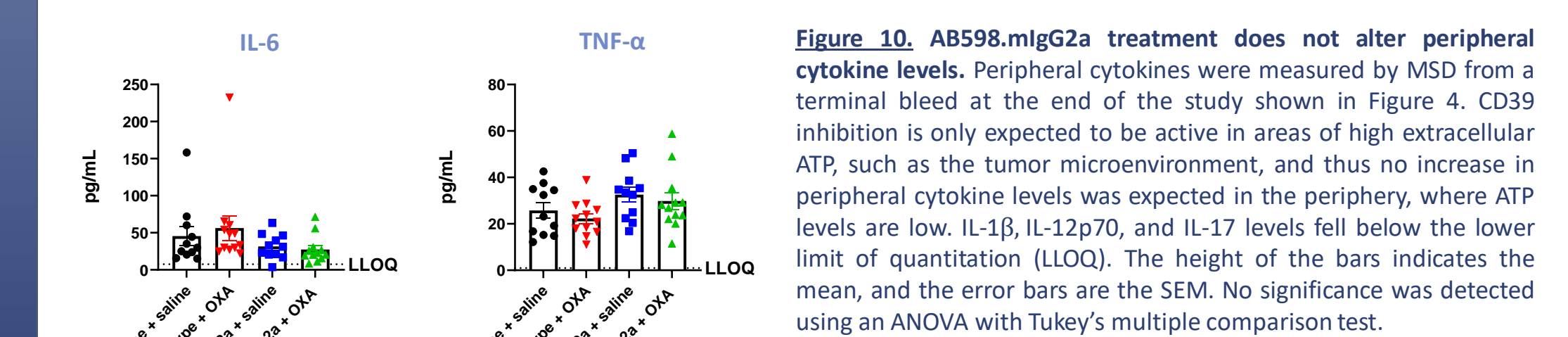


Figure 10. AB598.mlgG2a treatment does not alter peripheral cytokine levels. Peripheral cytokines were measured by MSD from a terminal bleed at the end of the study shown in Figure 4. CD39 inhibition is only expected to be active in areas of high extracellular ATP, such as the tumor microenvironment, and thus no increase in peripheral cytokine levels was expected in the periphery, where ATP levels are low. IL-1β, IL-12p70, and IL-17 levels fell below the lower limit of quantitation (LLOQ). The height of the bars indicates the mean, and the error bars are the SEM. No significance was detected using an ANOVA with Tukey's multiple comparison test.

CONCLUSION

- Our results indicate the superb ability of AB598.mlgG2a to inhibit intratumoral CD39 enzymatic activity, resulting in tumor growth inhibition. The findings presented here provide a rationale for the combination of CD39 inhibition with ICD-inducing chemotherapy in the clinic.

CONTACT: Christine Bowman, PhD, cbowman@arcusbio.com